Int. J. Electrochem. Sci., 17 **(2022)** Article Number: 220426, doi: 10.20964/2022.04.06

International Journal of
ELECTROCHEMICAL
SCIENCE
www.electrochemsci.org

Electrochemical Detection of Gallic Acid in Green Tea Using Molecularly Imprinted Polymers on TiO_2@CNTs Nanocomposite Modified Glassy Carbon Electrode

Fengxian Qin[1,], Tiejun Hu[2,*], Lixin You[1], Wei Chen[1], Dongshu Jia[1], Nannan Hu[1], Weihua Qi[1]*

[1] School of Life Sciences, Changchun Sci-Tech University, Changchun 130-600, China
[2] Deer Industry Engineering Research Center, Changchun Sci-Tech University, Changchun 130-600, China
[*]Correspondence E-mail: zhushikunmama@sina.com

Received: 13 December 2021 / *Accepted:* 27 January 2022 / *Published:* 4 March 2022

The purpose of this study was to use molecularly imprinted polymers on a TiO_2@CNTs nanocomposite modified glassy carbon electrode (MIP/TiO_2@CNTs/GCE) to electrochemically determine gallic acid (GA) in green tea. The TiO_2@CNTs nanocomposite was used to modify the GCE surface using the electrodeposition method and MIP was electropolymerized on the nanocomposite modified GCE. The successful electrodeposition of TiO_2@CNTs nanocommposite on GCE and the electropolymerization of the MIP layer on the nanocommposite surface were demonstrated by structural investigations using SEM and XRD. The MIP/TiO2@CNTs/GCE was found to be a stable and selective GA electrochemical sensor with a concentration range of 50–700 µM, a sensitivity of 0.02348µA/µM, and a limit of detection (LOD) of 12 nM in electrochemical tests employing DPV experiments. A comparison of the performance of MIP/TiO_2@CNTs/GCE with that of existing GA electrochemical sensors revealed that the suggested sensor had improved performance, a larger linear range, and an acceptable LOD value for GA detection. The precision and applicability of the proposed electrochemical GA sensor were investigated for determining the level of GA in a prepared real sample of green tea, and the results showed that RSD (2.86% to 4.20%) and recovery (97.65% to 99.30%) of spiked levels in a prepared real sample were acceptable, indicating that MIP/TiO_2@CNTs/GCE can be considered a reliable GA sensor in food samples.

Keywords: Gallic acid; Differential pulse voltammetry; Molecularly imprinted polymers; Nanocomposite; TiO_2; CNTs; Green tea

1. INTRODUCTION

Gallic acid (GA, $C_7H_6O_5$) is a phenolic acid present in organic plants, including fruits, nuts, wine, and tea. GA is a bioactive compound that exhibits antioxidant properties through cytotoxicity

against cancer cells while causing no harm to healthy cells [1, 2]. It helps to protect our cells from oxidative damage and may have health benefits such as antimicrobial, anti-inflammatory, and anti-obesity properties that could improve cancer and brain health, as well as therapeutic activities in gastrointestinal, neuropsychological, metabolic, and cardiovascular disorders [3, 4]. It's also commonly used as a distant astringent in the treatment of internal bleeding [5, 6]. GA has been demonstrated in studies to be effective in the treatment of albuminuria and diabetes [7-9]. It also possesses skin-brightening, anti-inflammatory, and photoprotective effects, all of which work to prevent pigmentation and keep the skin looking bright and even [10].

The GA potential for application in clinical and food requires identifying the rich source of GA in plants. Extraction and determination of the GA level are important [11, 12]. Accordingly, many studies have been carried out using colorimetry [13], chemiluminescent [14], high-performance liquid chromatography [15], spectrophotometry [16], UV [17], Folin–Ciocalteu assay [18], and electrochemical techniques [19-27]. Electrochemical techniques, which are simple, low-cost, and fast, can be used to detect a wide range of organic and inorganic analytes [28, 29]. The sensitivity and selectivity of electrochemical sensors can be enhanced using suitable nanostructured composites and hybrid materials. Therefore, this study focused on the electrochemical determination of GA in green tea using a MIP/TiO_2@CNTs modified electrode.

2. EXPERIMENTAL

2.1. Preparation of MIP/TiO_2@CNTs/GCE

GCE was meticulously polished using alumina slurries with a particle size of 0.05m (99%, Sigma-Aldrich) before modification to achieve a mirror finish. The GCE was then ultrasonically cleaned for 3 minutes in deionized water. GCE cleaning was followed by electrochemical activation using the CV technique in 0.1M H_2SO_4 (97%, Merck, Germany) solution at a scan rate of 50mV/s on an Autolab potentiostat-galvanostat model PGSTAT30 (Autolab, Netherlands) with a three-electrode system: GCE working electrode, platinum plate counter electrode, and an Ag/AgCl reference electrode. For electrodeposition of TiO_2@CNTs nanocommposite on clean GCE, the CNTs (99%, Guangzhou Hongwu Material Technology Co. Ltd., China) were ultrasonically functionalized in a solution of 1.0 M H_2SO_4 and I.0 M HNO_3 (99%, Xinxiang Omao Chemical Co., Ltd., China) with a ratio of 3:1 for 5 hours, and then washed with deionized water. Sequently, 1 g/l suspension of functionalized CNTs were added to electrolyte consisting of 10 mM $Ti(SO_4)_2$ (≥99%, Sigma-Aldrich), 10 mM H_2O_2 (99%, Shanghai Yunhong New Material Co., Ltd., China) and 3 M KCl (99.5%, Inner Mongolia Pulis Chemical Co., Ltd., China), and electrodeposition was performed using CV technique in prepared electrolyte in potential range from −0.8 to 0.8 V at a scan rate of 50 mV/s for 30 cycles [30]. Afterwards, the MIP film was electropolymerized on TiO_2@CNTs nanocommposite modified GCE using the CV technique in a potential range from 0.0 to 0.8 V at a scan rate of 50 mV/s for 30 cycles in an electrolyte prepared from 0.6 ml methacrylic acid (MAA, Jinan Future Chemical Co., Ltd., China) as a monomer, 70.0 ml of dry chloroform (≥99%, Sigma-Aldrich), 40.0 ml ethylene glycol

dimethacrylate (EDMA, 95%, Sigma-Aldrich) and 4 mg of 2,2-azobis -2-methyl propionitrile (AMP, 98%, Sigma-Aldrich) [21, 31].

2.2. Characterization

The morphological and crystallographic examinations of the materials were performed using a scanning electron microscope (SEM; Hitachi S-4500, Japan) and an X-ray diffractometer (XRD; Schimadzu model: XRD 6000 with CuK radiation, Japan). The Autolab potentiostat-galvanostat system was used to perform differential pulse voltammetry (DPV) measurements. For electrochemical investigations, a 0.1M phosphate buffer solution (PBS, Sigma-Aldrich) with a pH of 7.4 was utilized as the electrolyte.

2.3. Preparation of a real sample of green tea

For the preparation of the real sample, local green tea drinks were purchased from a local market, filtered, and centrifuged at 1000 rpm for 5 minutes. The supernatant was used for the preparation of the 0.1 M PBS with pH 7.4. Then, the DPV analysis was applied to determine the GA level in the prepared real sample. Moreover, the recovery and relative standard deviation (RSD) values were determined using the standard addition method.

3. RESULTS AND DISCUSSION

3.1. SEM and XRD analyses

SEM images of electrodeposited CNTs, TiO_2@CNTs and MIP/TiO_2@CNTs on GCE surfaces are depicted in Figure 1. The morphology of CNTs shows that the CNTs with rod structures are electrodeposited at rather uniform diameters (∼50 nm) on GCE. The CNTs are randomly oriented and some of them are entangled. Compared with the electrodeposited CNTs shown in Figure 1a, the TiO_2@CNTs nanocomposite preserves the 1D nanostructure of the CNTs, and the surfaces of the CNTs become coarse, implying the anchoring of TiO_2 NPs with an average diameter of 65 nm on the CNTs. The SEM image of the MIP/TiO_2@CNTs/GCE reveals that the MIP thin film was continuously wrapped on the TiO_2@CNTs nanocomposite and increased the diameter of the rod structures to ∼70 nm.

In Figure 2, XRD patterns of powders of electrodeposited CNTs, TiO_2@CNTs and MIP/TiO_2@CNTs on GCE surfaces are exhibited. The XRD pattern of CNTs displays that there are four characteristic diffraction peaks at 2θ= 25.92°, 43.91°, 51.04° and 72.65° corresponding to (002), (101), (004) and (110) planes of CNTs, respectively (JCPDS card No. 41-1487). The XRD pattern of TiO_2@CNTs shows diffraction peaks of (002) and (101) of CNTs, and additional diffraction peaks 2θ= 25.31°, 37.63°, 47.77°, 53.62°, 55.19°, 62.62°, 68.62°, 70.03° and 74.89° corresponding to (101),

(004), (200), (105), (211), (204), (116), (120) and (215) planes of the anatase phase of TiO_2, respectively (JCPDS card No. 01-084-1286).

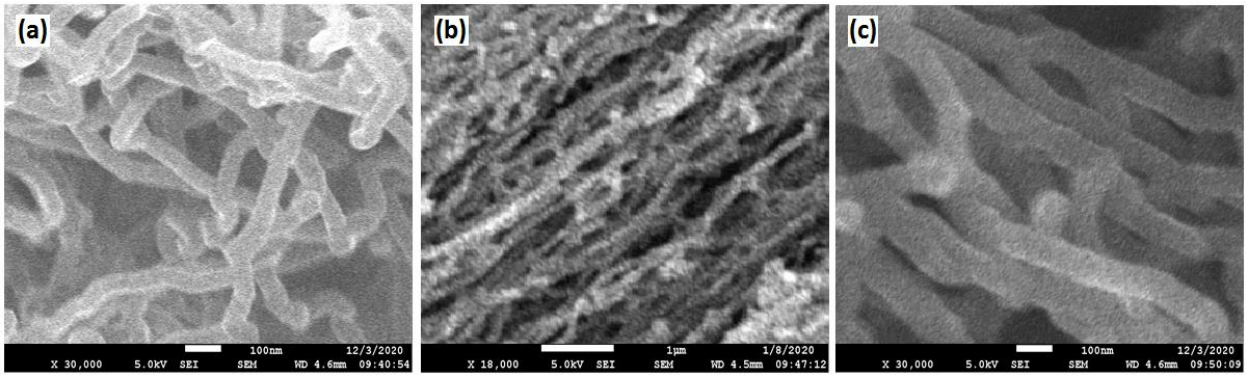

Figure 1. SEM images of electrodeposited a) CNTs, (b)TiO_2@CNTs and (c) MIP/TiO_2@CNTs on GCE surfaces.

The XRD patterns of powders of electrodeposited MIP/TiO_2@CNTs also shows the same diffraction peaks toward TiO_2@CNTs but the intensities of diffraction peaks in MIP/TiO_2@CNTs are decreased as compared to those of TiO_2@CNTs and CNTs. It can be related to the X-ray beam scattering ability of MIP and its amorphous nature [32, 33]. These observations in SEM and XRD analyses are good indications of the successful electrodeposition of TiO_2@CNTs nanocommposites on GCE and the electropolymerization of the MIP layer on the TiO_2@CNTs nanocommposite surface.

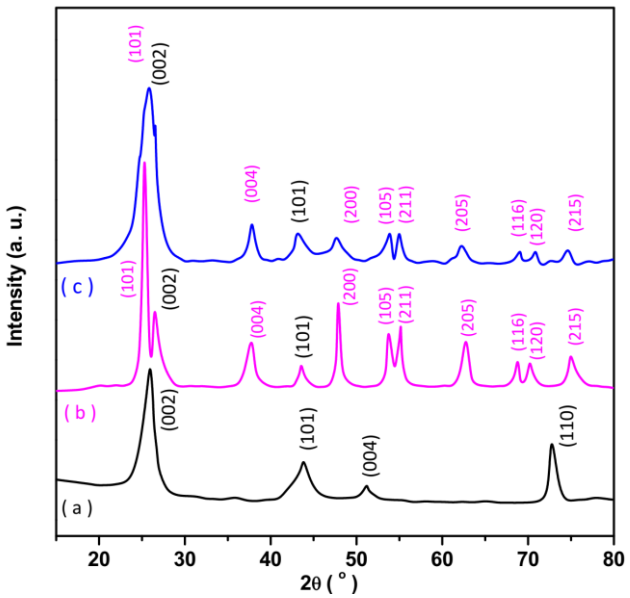

Figure 2. XRD patterns of powders of electrodeposited (a) CNTs, (b)TiO_2@CNTs and (c) MIP/TiO_2@CNTs on GCE surfaces.

3.2. Electrochemical analyses

The electrochemical behavior of bare GCE and modified GCE in the absence and presence of GA is studied using the DPV technique in 0.1M PBS with pH 7.4 at the potential range from -0.2V to 0.6V at a 50mV/s scan rate. In the absence of GA, Figure 3 shows that the DPV responses of electrodes do not exhibit the obvious peak. However, the addition of 150 µl GA solution, the anodic peaks at 0.20 are observed for all electrodes. The highest current density is observed for MIP/TiO_2@CNTs/GCE and it is attributed to the modification of the electrode with MIP which contained recognition sites and the higher adsorption ability for GA [34-36]. The recognition sites are exposed on the surface of the MIP, resulting in an increase in the mass-transfer rate and efficiency. CNTs increase the number of MIP recognition sites due to the high specific surface area of CNTs [37, 38]. The functionalized CNTs have been exploited in conjunction with MIPs to improve conductivity and facilitate the electron transfer rate [39]. Moreover, the MIP have been implanted with electrochemically active TiO_2 NPs for effective determination of GA by the concept of molecular imprinting [40]. TiO_2 NPs surfaces modified with MIP can not only make nanostructures more compatible with polymer matrix and increase binding rate, but also change their hydrophobic or hydrophilic character [40, 41]. These changes introduce new functional groups for the reaction with organic molecules [41, 42]. Thus, composite tailor-made receptors can be favorably oriented to bind with target moieties and reduce non-specific adsorption [43]. The oxidation profile of GA is electrochemically explained by the formation of the semi Quinone radical by the galloyl group oxidation as presented in Figure 4 [44-46].

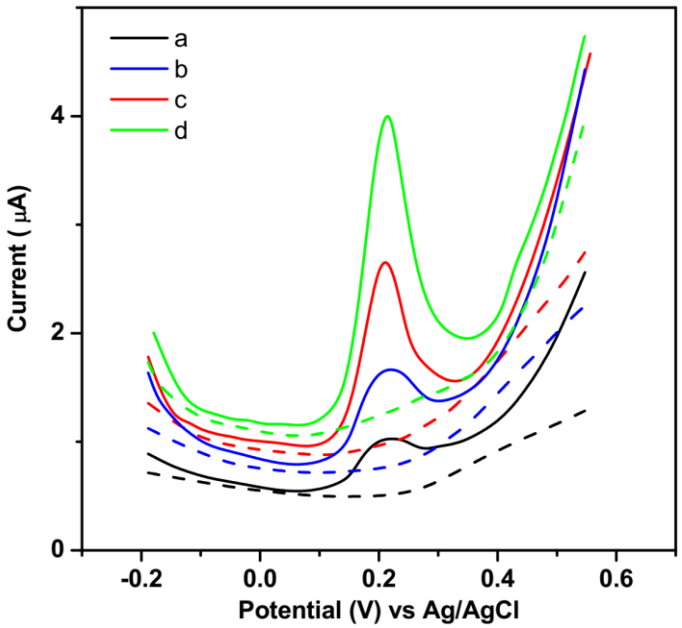

Figure 3. The electrochemical behavior of (a) bare GCE, (b) CNTs/GCE, (c) TiO_2@CNTs/GCE and (d) MIP/TiO_2@CNTs/GCE and modified GCE in absence (dashed line) and presence of (solid line) 150 µl GA using DPV technique in 0.1M PBS with pH 7.4 at the potential range from -0.2V to 0.6V at 50mV/s scan rate.

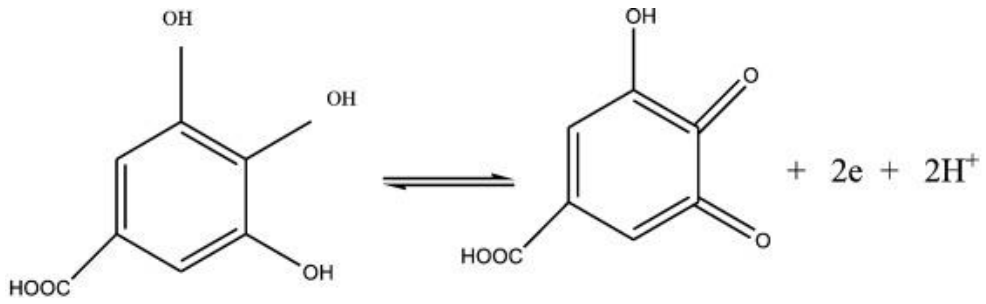

Figure 4. Schematic image for oxidation of GA on electrode surfaces [44].

Further electrochemical studies were performed on the evaluation of the stability of the electrochemical response of bare and modified GCE. Figure 5 shows the resultant first and 100th DPV curves of all electrodes in 0.1 M PBS with pH 7.4 containing 150 µl GA solution at the potential range from -0.2 V to 0.6 V at a scan rate of 50 mV/s. As observed, that the first DPV curve and the resulted DPV response after successive 100 scans are indicated to be 15%, 9%, 6% and 3% decrease for the current peak of GCE, CNTs/GCE, TiO_2@CNTs/GCE and MIP/TiO_2@CNTs/GCE, respectively. It is demonstrated that the high stability of the electrochemical response of MIP/TiO_2@CNTs/GCE due to the successful electropolymerization of MIPs that mainly depends on the stability and strength of the monomer and binding interactions between the template and monomer [47-49]. Therefore, the following electrochemical experiments were performed using MIP/TiO_2@CNTs/GCE.

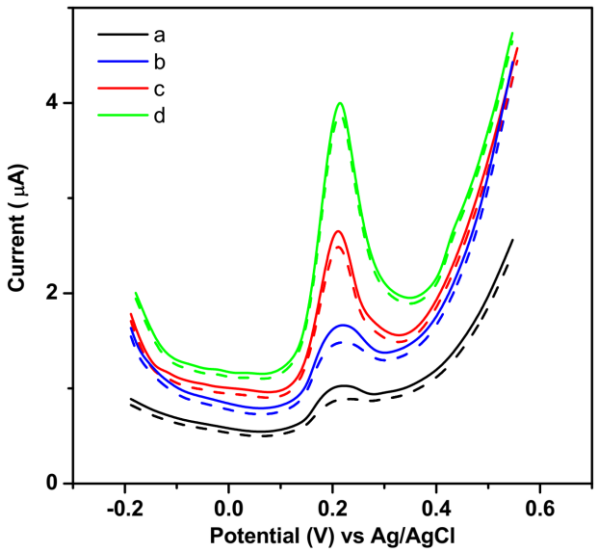

Figure 5. The resulted first (solid line) and 100th (dashed line) DPV curves of electrodes in 0.1 M PBS with pH 7.4 containing 150 µl GA solution at the potential range from -0.2V to 0.6V at 50mV/s scan rate.

Figure 6 exhibits the DPV response of MIP/TiO_2@CNTs/GCE to consecutive injections of 50 µM GA solution in 0.1M PBS with pH 7.4 at the potential range from -0.2V to 0.6V at 50mV/s scan

rate. It can be observed that the addition of a 50 µM GA electrochemical cell provides an increase in the DPV current intensity. The inset of Figure 6 depicts the calibration plot curve regarding the DPV response of the developed GA electrochemical sensor with a concentration range of 50–700 µM, and a sensitivity of 0.02348µA/µM. The results demonstrated that LOD estimated based on signal to noise ratio (S/N = 3), was found to be 12 nM. A performance comparison between MIP/TiO_2@CNTs/GCE and some other GA electrochemical sensors is summarized in Table 1. The results illustrate that the proposed sensor in this study has better performance, a wider linear range and an acceptable LOD value for GA detection. It is associated with the high surface area of TiO_2@CNTs nanocomposite, which acts as high-surface 3D scaffolds for the deposition of thin MIP layers and improves electron and charge transfer abilities between the porous surface of the electrode and analyte molecules in the electrolyte [50]. Furthermore, the chemical stability and high mechanical strength of MIP and TiO_2@CNTs nanocomposite materials benefit the diffusion of reacting agents.

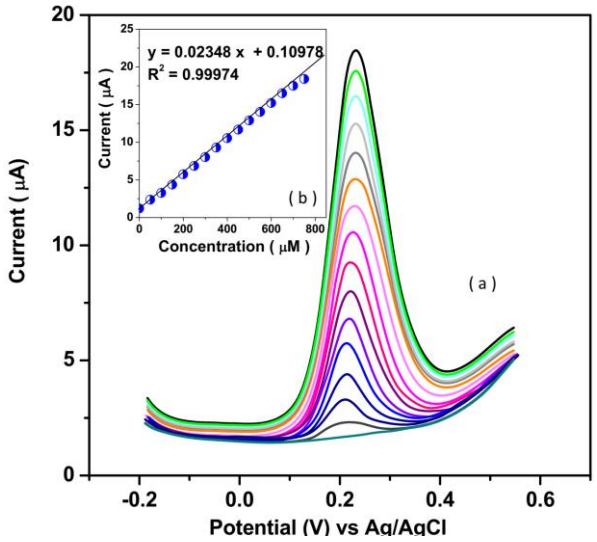

Figure 6. DPV response of MIP/TiO_2@CNTs/GCE to consecutive injections of 50 µM GA solution in 0.1M PBS with pH 7.4 at the potential range from -0.2V to 0.6V at 50mV/s scan rate.

Table 1. A performance comparison between MIP/TiO_2@CNTs/GCE and some other GA electrochemical sensors.

Electrodes	Technique	LOD (nM)	Linear range (µM)	Ref.
MIP/TiO_2@CNTs/GCE	DPV	12	50 to 700	This work
polyepinephrine/GCE	DPV	663	1.0 to 20	[19]
MIP/MWCNT/ carbon paste electrode	DPV	47	0.12 to 380	[21]
SiO_2 NPs/ carbon paste electrode	DPV	800	0.8 to 100	[22]
CS/ functionalized Fe_2O_3/ERGO/GCE	DPV	150	1 to 100	[20]
Au microclusters/ sulfonate functionalized graphene /GCE	DPV	10.7	0.05 to 8.0	[25]

Ag NPs/ delphinidin/GCE	AMP	280	8.68 to 625.80	[24]
Glutamic acid/rGO/paraffin impregnated graphite electrode	AMP	10	0.03 to 480	[23]
Bi-MWCNT/carbon paste electrode	AMP	160	1 to 100	[51]
poly(melamine)/screen-printed carbon electrode	FIA	210	1 to 1000	[52]

AMP : Amperometry ; FIA: flow-injection amperometry

The specificity of MIP/TiO_2@CNTs/GCE to determination of GA was examined in the present of some organic and inorganic substances as major compounds in green tea. Table 2 presents the results of electrocatalytic current of DPV measurement in 0.1M PBS with pH 7.4 at the potential range from -0.2V to 0.6V at a 50mV/s scan rate to successive injections of 10 µM GA solution and 30 µM of substances. As can be seen, the electrocatalytic response of MIP/TiO_2@CNTs/GCE to the addition of GA solution is remarkable significant, and an insignificant response is observed for these substances, indicating that these compounds have no significant interference for the voltammetric determination of GA using the proposed procedure. It is concluded that the proposed method can be considered specific [53]. The polymer scaffold of the MIP MIPs as a recognition element provides specificity by substrate binding to the cavities and target analytes to generate an electrochemical signal [54, 55].

Table 2. Results of electrocatalytic current of DPV measurement in 0.1M PBS with pH 7.4 at the potential range from -0.2V to 0.6V at 50mV/s scan rate to successive injections of 10 µM GA solution and 30 µM of substances.

Substance	**Added (µM)**	**Electrocatalytic current (µA) at 0.2V**	**RSD (%)**
GA	10	0.2351	±0.0847
Catechin	30	0.0976	±0.0094
Phenolic acid	30	0.0281	±0.0038
B-carotene	30	0.0733	±0.0051
Tyrosine	30	0.0317	±0.0022
Glucose	30	0.0126	±0.0022
Theanine	30	0.0425	±0.0028
Caffeine	30	0.0851	±0.0088
Fluorine	30	0.0664	±0.0056
γ-aminobutyric acid	30	0.0822	±0.0083
Vitamin C	30	0.0612	±0.0064
Ca^{2+}	30	0.0093	±0.0038
Mn^{2+}	30	0.0820	±0.0043
Mg^{2+}	30	0.0511	±0.0082
Cu^{2+}	30	0.0288	±0.0071
K^{+}	30	0.0799	±0.0066
Zn^{2+}	30	0.0277	±0.0078

The precision and applicability of the proposed electrochemical GA sensor for determining the level of GA in a prepared real sample of green tea were investigated. Figure 7a shows the DPV response of MIP/TiO_2@CNTs/GCE to consecutive injections of 100 µM GA solution in a prepared real sample in 0.1M PBS with pH 7.4 at the potential range from -0.2V to 0.6V at 50mV/s scan rate. The resultant calibration curve in Figure 7b illustrates that the GA concentration in the prepared sample is 29.94 µM which is close to the reported GA content in green tea [56, 57]. Table 3 also exhibits the acceptable values for RSD (2.86% to 4.20%) and recovery (97.65% to 99.30%) of spiked levels in prepared real samples, which indicates that MIP/TiO_2@CNTs/GCE can be considered a reliable GA sensor in food samples.

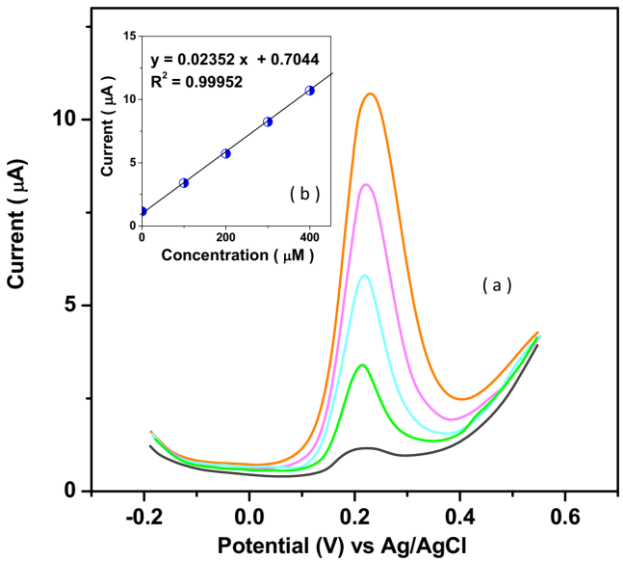

Figure 7. (a) DPV response of MIP/TiO_2@CNTs/GCE and (b) calibration curve to consecutive injections of 100 µM GA solution in prepared real sample in 0.1M PBS with pH 7.4 at the potential range from -0.2V to 0.6V at 50mV/s scan rate.

Table 3. Analytical findings of MIP/TiO2@CNTs/GCE to detection GA in prepared real samples of green tea.

Spiked (µm)	Detected (µm)	Recovery (%)	RSD (%)
100.0	98.6	98.60	3.17
200.0	195.3	97.65	2.86
300.0	297.9	99.30	3.58
400.0	392.5	98.12	4.20

4. CONCLUSION

In summary, this work presented the synthesis of MIP/TiO_2@CNTs/GCE using electrodeposition and electropolymerization for the electrochemical determination of GA in green tea.

Results of structural analyses indicated the successful electrodeposition of TiO_2@CNTs nanocommposite on GCE and electropolymerization of the MIP layer on the nanocommposite surface. Results of electrochemical studies showed that MIP/TiO_2@CNTs/GCE was performed as a stable and selective GA electrochemical sensor with a wide concentration range of 50-700 μM, and with acceptable values of sensitivity and LOD of 0.02348μA/μM and 12nM, respectively. The precision and applicability of the proposed electrochemical GA sensor were explored for the determination level of GA in prepared real sample of green tea. The results exhibited the acceptable values for RSD and recovery of spiked levels in a prepared real sample, which demonstrated that MIP/TiO_2@CNTs/GCE can be considered to a reliable GA sensor in food samples.

References

1. W. Zhu, M. Deng, D. Chen, Z. Zhang, W. Chai, D. Chen, H. Xi, J. Zhang, C. Zhang and Y. Hao, *ACS Applied Materials & Interfaces*, 12 (2020) 32961.
2. H. Maleh, M. Alizadeh, F. Karimi, M. Baghayeri, L. Fu, J. Rouhi, C. Karaman, O. Karaman and R. Boukherroub, *Chemosphere*, (2021) 132928.
3. N. Kahkeshani, F. Farzaei, M. Fotouhi, S.S. Alavi, R. Bahramsoltani, R. Naseri, S. Momtaz, Z. Abbasabadi, R. Rahimi and M.H. Farzaei, *Iranian Journal of Basic Medical Sciences*, 22 (2019) 225.
4. Y. Xie, X. Meng, Y. Chang, D. Mao, Y. Yang, Y. Xu, L. Wan and Y. Huang, *Composites Science and Technology*, 219 (2021) 109225.
5. Z. Zhang, L. Feng, H. Liu, L. Wang, S. Wang and Z. Tang, *Inorganic Chemistry Frontiers*, 9 (2022) 35.
6. Z. Wang, L. Dai, J. Yao, T. Guo, D. Hrynsphan, S. Tatsiana and J. Chen, *Bioresource Technology*, 327 (2021) 124785.
7. M.S. Garud and Y.A. Kulkarni, *Chemico-biological interactions*, 282 (2018) 69.
8. Y. Liu, Q. Zhang, H. Yuan, K. Luo, J. Li, W. Hu, Z. Pan, M. Xu, S. Xu and I. Levchenko, *Journal of Alloys and Compounds*, 868 (2021) 158723.
9. H. Guan, S. Huang, J. Ding, F. Tian, Q. Xu and J. Zhao, *Acta Materialia*, 187 (2020) 122.
10. X. Zhang, X. Sun, T. Lv, L. Weng, M. Chi, J. Shi and S. Zhang, *Journal of Materials Science: Materials in Electronics*, 31 (2020) 13344.
11. X. Du, W. Tian, J. Pan, B. Hui, J. Sun, K. Zhang and Y. Xia, *Nano Energy*, 92 (2022) 106694.
12. L. Zhang, M. Cong, X. Ding, Y. Jin, F. Xu, Y. Wang, L. Chen and L. Zhang, *Angewandte Chemie*, 132 (2020) 10980.
13. C. Dong, G. Wu, Z. Wang, W. Ren, Y. Zhang, Z. Shen, T. Li and A. Wu, *Dalton Transactions*, 45 (2016) 8347.
14. X. Wang, J. Wang and N. Yang, *Food chemistry*, 105 (2007) 340.
15. H. Wang, K. Helliwell and X. You, *Food Chemistry*, 68 (2000) 115.
16. J. Pooralhossini, M. Ghaedi, M.A. Zanjanchi and A. Asfaram, *Ultrasonics sonochemistry*, 34 (2017) 692.
17. F.H. Fernandes, R.S.d.A. Batista, F.D.d. Medeiros, F.S. Santos and A.C. Medeiros, *Revista Brasileira de Farmacognosia*, 25 (2015) 208.
18. M.-R. Gao, Q.-D. Xu, Q. He, Q. Sun and W.-C. Zeng, *Journal of Food Measurement and Characterization*, 13 (2019) 1349.
19. R. Abdel-Hamid and E.F. Newair, *Journal of Electroanalytical Chemistry*, 704 (2013) 30.

20. F. Gao, D. Zheng, H. Tanaka, F. Zhan, X. Yuan, F. Gao and Q. Wang, *Materials Science and Engineering: C*, 57 (2015) 279.
21. S. Shojaei, N. Nasirizadeh, M. Entezam, M. Koosha and M. Azimzadeh, *Food Analytical Methods*, 9 (2016) 2721.
22. J. Tashkhourian and S.F. Nami-Ana, *Materials Science and Engineering: C*, 52 (2015) 103.
23. J.J. Feminus, R. Manikandan, S.S. Narayanan and P. Deepa, *Journal of Chemical Sciences*, 131 (2019) 11.
24. M. Ghaani, N. Nasirizadeh, S.A.Y. Ardakani, F.Z. Mehrjardi, M. Scampicchio and S. Farris, *Analytical Methods*, 8 (2016) 1103.
25. Z. Liang, H. Zhai, Z. Chen, H. Wang, S. Wang, Q. Zhou and X. Huang, *Sensors and Actuators B: Chemical*, 224 (2016) 915.
26. M. Chen, H. Lv, X. Li, Z. Tian and X. Ma, *International Journal of Electrochemical Science*, 14 (2019) 4852.
27. T.-W. Chen, S. Palanisamy, S.-M. Chen, V. Velusamy and S.K. Ramaraj, *International Journal of Electrochemical Science*, 12 (2017) 4107.
28. R. Zhang, W. Zhang, M. Shi, H. Li, L. Ma and H. Niu, *Dyes and Pigments*, (2021) 109968.
29. M. Khosravi, *Journal of Eating Disorders*, 8 (2020) 1.
30. J. Tashkhourian, S.N. Ana, S. Hashemnia and M. Hormozi-Nezhad, *Journal of Solid State Electrochemistry*, 17 (2013) 157.
31. Y. Peng, Z. Wu and Z. Liu, *Analytical Methods*, 6 (2014) 5673.
32. T. Sajini, R. Thomas and B. Mathew, *Chinese Journal of Polymer Science*, 37 (2019) 1305.
33. S. Khosravi and S.M.M. Dezfouli, *Systematic Reviews in Pharmacy*, 11 (2020) 913.
34. S. Pardeshi, R. Dhodapkar and A. Kumar, *Adsorption Science & Technology*, 30 (2012) 23.
35. X. Zhang, Y. Tang, F. Zhang and C.S. Lee, *Advanced Energy Materials*, 6 (2016) 1502588.
36. A. Medghalchi, M. Akbari, Y. Alizadeh and R.S. Moghadam, *Journal of current ophthalmology*, 30 (2018) 353.
37. D.-L. Huang, R.-Z. Wang, Y.-G. Liu, G.-M. Zeng, C. Lai, P. Xu, B.-A. Lu, J.-J. Xu, C. Wang and C. Huang, *Environmental Science and Pollution Research*, 22 (2015) 963.
38. S.M.M. Dezfouli and S. Khosravi, *European Journal of Translational Myology*, 30 (2020) 291–296.
39. B. Hatamluyi, A. Hashemzadeh and M. Darroudi, *Sensors and Actuators B: Chemical*, 307 (2020) 127614.
40. L. Sun, J. Guan, Q. Xu, X. Yang, J. Wang and X. Hu, *Polymers*, 10 (2018) 1248.
41. K. Wieszczycka, K. Staszak, M.J. Woźniak-Budych, J. Litowczenko, B.M. Maciejewska and S. Jurga, *Coordination Chemistry Reviews*, 436 (2021) 213846.
42. M. Wang, C. Jiang, S. Zhang, X. Song, Y. Tang and H.-M. Cheng, *Nature chemistry*, 10 (2018) 667.
43. G.F. Abu-Alsoud, K.A. Hawboldt and C.S. Bottaro, *ACS applied materials & interfaces*, 12 (2020) 11998.
44. G. Ziyatdinova, E. Guss, E. Morozova, H. Budnikov, R. Davletshin, V. Vorobev and Y. Osin, *Food Analytical Methods*, 12 (2019) 2250.
45. S. Mu, Q. Liu, P. Kidkhunthod, X. Zhou, W. Wang and Y. Tang, *National Science Review*, 8 (2020) 1.
46. M. Khosravi, *Open Access Macedonian Journal of Medical Sciences*, 8 (2020) 553.
47. A. Martín-Esteban, *TrAC Trends in Analytical Chemistry*, 45 (2013) 169.
48. L. Zhou, *International Journal of Electrochemical Science*, 16 (2021) 211043.
49. S.M. Mahmoudinezhad Dezfouli and S. Khosravi, *Indian Journal of Forensic Medicine & Toxicology*, 15 (2021) 2674.
50. X. Yangli, M. Liuwei, C. Xiaojing, C. Xi, S. Laijin, Y. Leiming, S. Wen and G. Huang, *Plasma Science and Technology*, 23 (2021) 085503.

51. Madhusudhana, G. Manasa, A.K. Bhakta, Z. Mekhalif and R.J. Mascarenhas, *Materials Science for Energy Technologies*, 3 (2020) 174.
52. Y.-L. Su and S.-H. Cheng, *Analytica chimica acta*, 901 (2015) 41.
53. J. Shi, R. Rao, W. Tian, X. Xu and X. Liu, *Ceramics International*, 48 (2021) 5210.
54. A. Yarman and F.W. Scheller, *Sensors*, 20 (2020) 2677.
55. B. Cui, P. Liu, X. Liu, S. Liu and Z. Zhang, *Journal of Materials Research and Technology*, 9 (2020) 12568.
56. C. Asli, K. Batcioglu and E. Sarer, *Journal of Faculty of Pharmacy of Ankara University*, 44 (2020) 50.
57. J. Zhang, Y. Zhao, Y. Liu, C. Zhu, B. Wang, L. Zhang, G. Li, H. Wu, C. Liu and Y. Li, *Journal of Alloys and Compounds*, 902 (2022) 163723.